JOURNAL OF MATERIALS SCIENCE: MATERIALS IN MEDICINE **15** (2004) 1279–1284

Microwave accelerated synthesis of nanosized calcium deficient hydroxyapatite

A. SIDDHARTHAN[†,‡], S. K. SESHADRI[†], T. S. SAMPATH KUMAR*[,†,‡]
[†]*Department of Metallurgical and Materials Engineering and* [‡]*Sophisticated Analytical Instrumentation Facility, Indian Institute Technology Madras, Chennai – 600036, India*
E-mail: sampath@rsic.iitm.ernet.in

Rapid synthesis of calcium deficient hydroxyapatite (CDHA, $Ca_{10-x}(HPO_4)_x(PO_4)_{6-x}(OH)_{2-x}$) with Ca/P ratio 1.5 was done by precipitation using calcium nitrate tetra-hydrate and phosphoric acid and subsequently subjecting to microwave irradiation in a domestic microwave oven for 15 min. Transmission electron microscopy analysis shows needle like morphology of CDHA having length 16–39 nm and width 7–16 nm. The synthesized CDHA has the characteristic HPO_4^{2-} vibration band at 875 cm^{-1} in Fourier transform infrared (FT-IR) spectra. The X-ray powder diffraction (XRD) analysis shows a pattern corresponding to stoichiometric hydroxyapatite (HA) with broad peaks suggesting that CDHA particles were nanosized. Fourier transform Raman spectroscopy (FT-Raman) do not indicate any fluorescence band that is characteristic of non-stoichiometric HA. The thermal decomposition of CDHA to beta tricalcium phosphate (β-TCP) was also studied for the additional confirmation. The nanosized CDHA was found to be stable up to 600°C.

1. Introduction

Hydroxyapatite (HA, $Ca_{10}(PO_4)_6(OH)_2$) is one of the most important bioceramics for medical and dental applications as it is the main inorganic constituent of hard tissues like bone and teeth [1]. There is a great demand for this material in odontology and traumatology, together with other materials of calcium phosphate family such as beta tricalcium phosphate (β-TCP, $Ca_3(PO_4)_2$) and tetracalcium phosphate (TTCP, $Ca_4P_2O_9$) [2]. This arises from their ability to bond with bone mineral directly and to promote new bone formation by oestoconduction [3]. However, bone mineral is essentially calcium deficient hydroxyapatite (CDHA) with Ca/P ratio of about 1.5, which strictly speaking is chemically and compositionally similar to TCP while being structurally similar to stoichiometric HA (Ca/P = 1.67) [4]. Apatites with Ca/P ratios ranging from 1.67 to 1.33 originate from the loss of Ca^{2+} ions from the unit cell; hence the name calcium deficient hydroxyapatite with the formula $Ca_{10-x}(HPO_4)_x(PO_4)_{6-x}(OH)_{2-x}$ [5]. The HPO_4^{2-} formation results from the occupation by H_2O molecules at the vacant OH^- sites and hydrogen bonding to the nearest PO_4^{3-} groups as:

$$PO_4^{3-} + H_2O \rightarrow HPO_4^{2-} + OH^- \quad (1)$$

This class of compounds has lower stability than stoichiometric HA and above 200°C, the HPO_4^{2-} group begins to transform into $P_2O_7^{4-}$ by the reaction [6]:

$$2HPO_4^{2-} \rightarrow P_2O_7^{4-} + H_2O \quad (2)$$

The condensation process takes place over a wide range of temperatures and only above 300°C does the reaction go to completion. The CDHA with Ca/P ratio equal to 1.5 converts to β-TCP at temperatures lower than 900°C, whereas the same thermal treatment would result in an excess of either HA or calcium pyrophosphate (β-CPP, $Ca_2P_2O_7$), depending on the value of Ca/P (>1.5 or <1.5) [6]. Precipitated CDHA usually have a *c*-axis parameter similar to HA, but the *a*-axis parameter is typically increased by 0.01–0.02 Å [7], indicating that lattice substitutions do take place.

Naturally occurring CDHA play an important role in several processes such as bone remodeling and bone formation [4]. The CDHA seems to be more efficient in inducing the precipitation of bone-like apatite than stoichiometric HA [8]. CDHAs are highly soluble in water or body fluids whereas high crystalline stoichiometric HA exhibit low solubility [9]. CDHA has higher specific surface area compared to HA and TCP and have more reproducible seeding efficacy [10]. The calcium phosphates used for bone regeneration should have high bioactivity i.e., its ability to form bone-like apatite layer on its surface, which depend on the dissolution rate. CDHA possessing above attributes

*Author to whom all correspondence should be addressed.

has been utilized for bone substitution, implant coating, drug delivery etc. In addition, CDHA possess electrical properties sensitive to environment at high temperature, making them potential candidates for non-biological applications in gas sensors and proton conductors [11].

Biological apatites are nanostructured crystals of dimension 20 nm in diameter and 50 nm long. From bionics viewpoint, synthetic apatites to be used for repairing damaged hard tissues are expected to have characteristics closer to those of biological apatite in both composition and structure. Nanocrystalline HA has proved to be of greater biological efficacy in terms of osteoblast adhesion, proliferation, oesseointegration and formation of new bone on its surface [12]. Many methods have been reported for synthesizing CDHA [6, 13, 14] and these involve long durations for reaction, drying etc. Microwave plays an important role in reactions in aqueous media [15] and has been used for preparing HA in less than 45 min [16]. Precipitation of nanosized HA using microwave irradiation from citrate-phosphate solutions has been reported [17]. In this paper rapid synthesis of nanosized CDHA through the reaction of calcium nitrate tetra hydrate [$Ca_3(NO_4)_2{\cdot}4H_2O$] and phosphoric acid (H_3PO_4) by microwave irradiation is discussed.

2. Experimental details

A simple co-precipitation method was used to prepare nanosized CDHA powder using calcium nitrate tetra hydrate [$Ca_3(NO_4)_2{\cdot}4H_2O$] and phosphoric acid (H_3PO_4) as starting materials [18]. Calcium nitrate was dissolved in distilled water to form 0.5 M solution, into which phosphoric acid was added in order to obtain a Ca/P ratio of 1.5. After 30 min of mixing, ammonium hydroxide was added to the mixed solution. Stirring for further 30 min resulted in a precipitate which was washed repeatedly to remove unwanted ions (NH^{4+} and NO_3^{2-}). The precipitate in paste form was subjected to microwave irradiation in a domestic microwave oven (BPL India, 2.45 GHz, 800 W power) for 15 min. The CDHA powder was obtained by grinding using agate mortar and pestle.

A small quantity of the powder was heat treated at 100, 500, 550, 600, 650 and 700°C for 2 h in a muffle furnace to study thermal decomposition and phase changes that occur. The X-ray powder diffraction (XRD) analysis was done (Shimadzu, XD-D1, Japan) in reflection mode with Cu K_α radiation. The functional groups present in CDHA were ascertained by Fourier transform infrared spectroscopy (FT-IR) and Fourier transform Raman (FT-Raman) spectroscopy (Bruker IFS 66V FT-IR spectrometer, Germany equipped with FRA 106 Raman attachment). The FT-IR spectra were obtained over the region 400–4000 cm^{-1} using KBr pellet technique with spectral resolution of 4 cm^{-1}. The FT-Raman spectra were obtained in region of 50–3500 cm^{-1} with spectral resolution of 4 cm^{-1} by Nd: YAG laser excitation of wavelength 1064 nm. The crystalline size and morphology were analyzed in a transmission electron microscope (TEM) operated at 120 KeV (Philips CM12wSTEM, Netherlands). TEM specimens were prepared by depositing a few drops of CDHA dispersed in acetone on carbon coated copper grid.

3. Results and discussion

The XRD pattern of as synthesized CDHA, shown in Fig. 1, is typical of the pattern for HA in the absence of other phases. Even though the starting Ca/P ratio was 1.5 it has resulted in the formation of CDHA with the same XRD pattern of HA (JCPDS- 9-432) [6, 13, 14]. The broad peaks indicate nanocrystalline nature of synthesized powder. The average crystallite size of the powder was estimated using the Scherrer formula $t = K\lambda/B\,Cos\theta$, where t is the average crystallite size (nm); K is the shape factor ($K = 0.9$); λ is the wavelength of the X-rays ($\lambda = 1.54056$ Å for Cu K_α radiation); B is the full width at half maximum (radian) and θ is the Bragg's diffraction angle (°). The diffraction peak at 25.9° (2θ) was chosen for calculation of the crystalline size, as it is isolated from others. This peak corresponds to (002) Miller plane family. The crystallite size was found to be 36 nm. The cell parameters of CDHA were calculated by least-squares fit method and found to be: $a = 9.434$ Å and $c = 6.872$ Å, which were similar to the reported values of CDHA namely, $a = 9.438$ Å and $c = 6.886$ Å [20]. The increase in 'a' axis value as compared to the stoichiometric HA value of 9.418 Å may be due to lattice substitution of HPO_4^{2-} ions [7].

The CDHA samples heat treated at 500, 550 and 600°C doesn't show any intermediate phase like β-CPP but the crystallinity was found to be lower than that of stoichiometric HA [19]. The samples heat treated at 650 and 700°C shows pattern corresponding to β-TCP (JCPDS 9-169) alone with the absence of HA or β-CPP. This confirms that the Ca/P ratio of synthesized CDHA is 1.5 [6]. The $P_2O_7^{4-}$ would have reacted with OH^- to form PO_4^{3-} around 650°C [6]. CDHA has transformed to β-TCP at a temperature lower than reported [6] which may be due to the nanophasic nature of CDHA.

The FT-IR spectra of as synthesized and 100°C heat treated samples shown in Fig. 2 exhibit clear evidence of CDHA by the presence of HPO_4^{2-} ion bands [13, 14, 21]. As listed in Table I, the stretching and librational modes of OH^- groups and the internal modes corresponding to the PO_4^{3-} groups were observed similar to that of HA. The bands corresponding to adsorbed H_2O and CO_3^{2-} ions were also noted [21]. The CDHA also exhibit low intense OH^- stretching and librational bands than stoichiometric HA [22], which supports the loss of OH^- ions from the unit cell. The HPO_4^{2-} band was not observed for samples heat treated above 500°C. It has been reported that conversion of HPO_4^{2-} to $P_2O_7^{4-}$ occurs above 200°C. The sample heat treated at 500°C shows bands at 725 cm^{-1} which corresponds to $P_2O_7^{4-}$ vibrational band while it is not observed in heat treated samples above 500°C. This may be due to the loss of pyrophosphate through reaction with HA to form β-TCP [6]. These changes appear to have taken place

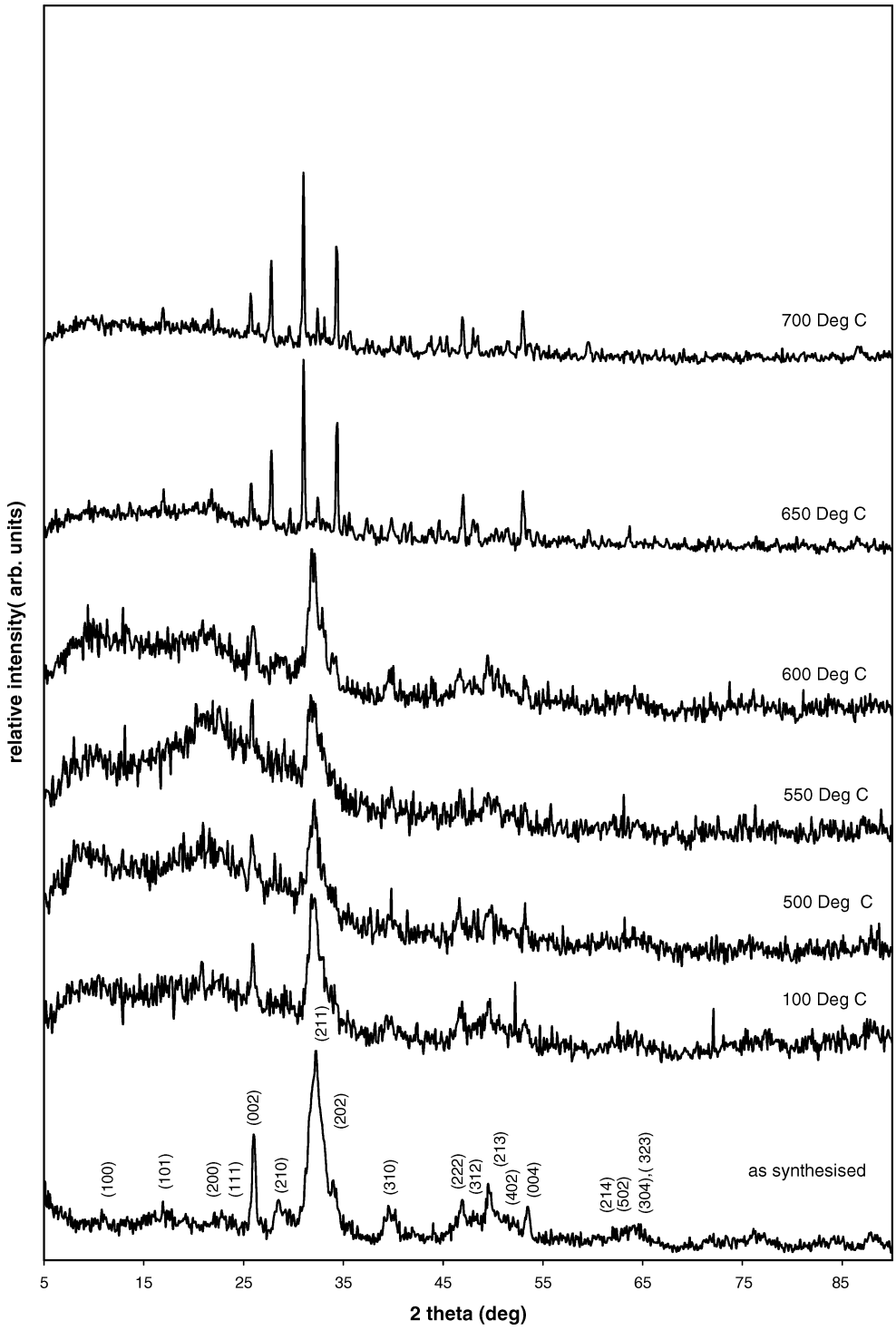

Figure 1 XRD pattern of as synthesized CDHA and heat treated samples.

in the apatitic structure as it was undetected in XRD patterns of samples heat treated at 500, 550 and 600°C [6].

The intensities of both the hydroxyl and phosphate bands can be used as an indication of the HA crystallinity [23]. The heat treated samples exhibits low intensity of the above bands which corroborate with the XRD results suggesting low crystallinity of CDHA. The samples heat treated at 650 and 700°C shows bands at 947, 986 and 1122 cm^{-1} corresponding to β-TCP [21] and absence of OH^- band. All CDHA samples showed broad bands corresponding to adsorbed water. This may arise due to nanoparticle nature and associated porosities resulting in adsorbed water peak at higher temperatures [23].

Fig. 3 shows that FT-Raman spectra of as synthesized CDHA and 100°C heat treated sample have characteristic bands at 964 and 1046 cm^{-1} of P─O bond stretching and 594 and 433 cm^{-1} of O─P─O bending of PO_4^{3-} group of HA [21]. The slight deviation from reported value arises from HPO_4^{2-} ions present in CDHA samples. The absence of fluorescence band around 770–690 cm^{-1} [24] arising from hexagonal structure of stoichiometric HA is clear evidence of perturbed structure of CDHA due to incorporation of HPO_4^{2-} ion. The result is in accordance with cell parameters calculated

TABLE I Assignments of infrared frequencies (cm^{-1}) of as synthesized CDHA and heat treated samples

	Infrared frequencies (cm^{-1})						
	CDHA					β−TCP	
Assignments	as synthesized	100°C	500°C	550°C	600°C	650°C	700°C
PO_4^{3-} bend ν_2	471	471	473	472	472	–	–
PO_4^{3-} bend ν_4	564	564	565	566	567	554	552
PO_4^{3-} bend ν_4	603	603	602	602	602	606	608
Structural OH^-	633	633	634	631	631	–	–
$P_2O_7^{4-}$	–	–	725	–	–	–	–
HPO_4^{2-}	875	875	–	–	–	–	–
PO_4^{3-} stretch ν_1	962	962	962	962	962	947	943
PO_4^{3-} stretch ν_1	–	–	–	–	–	985	986
PO_4^{3-} bend ν_3	1034	1034	1042	1043	1044	1045	1042
PO_4^{3-} bend ν_3	–	–	1092	1091	1091	1070	1072
HPO_4^{2-}	1094	1094	–	–	–	–	–
PO_4^{3-} bend ν_3	–	–	–	–	–	1122	1119
CO_3^{2-} ν_3	1402	–	–	–	–	–	–
CO_3^{2-} ν_3	1455	–	–	–	–	–	–
H_2O adsorbed ν_2	1641	1632	1632	1642	1642	1642	1643
H_2O adsorbed	3400	3400	3400	3400	3400	3400	3400
Structural OH^-	3569	3570	3570	3570	3570	–	–

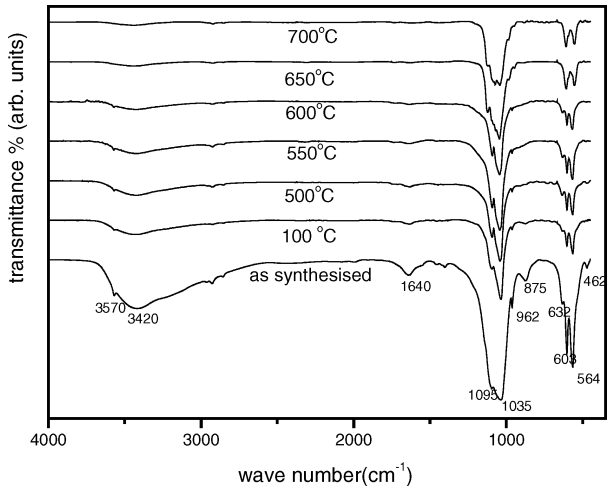

Figure 2 FT-IR spectra of as synthesized CDHA and heat treated samples.

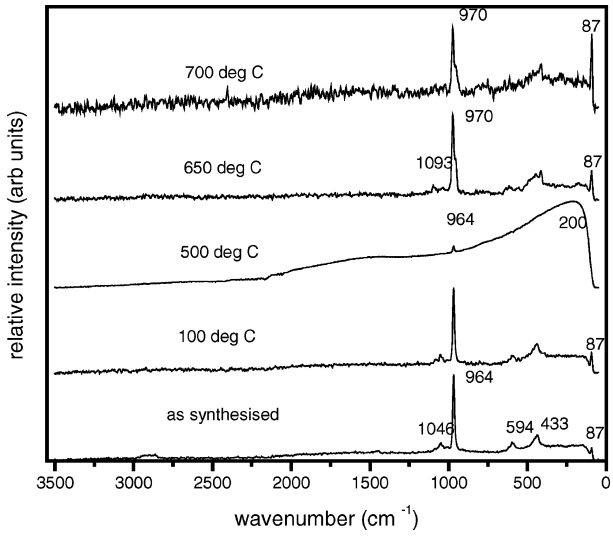

Figure 3 FT-Raman spectra of as synthesized CDHA and heat treated samples.

from XRD data. The sample heated at 500°C shows a very small band at 964 cm^{-1} and a large broad band at 200 cm^{-1} may be characteristic of $P_2O_7^{4-}$ formed as intermediate compound in hexagonal structure. The sample heat treated at 650 and 700°C show bands at 970, 1093 and a shoulder peak at 964 cm^{-1} for P─O stretching and a peak at 409 cm^{-1} for O─P─O bending mode of PO_4^{3-} group of β-TCP [21]. The lower crystallinity is characterized by lattice modes at 87 cm^{-1} and its intensity increases with crystallinity as shown by the samples heat treated at 650 and 700°C [24].

Both the bright and dark field TEM images and selected area electron diffraction (SAED) pattern of as synthesized CDHA particles are shown in Fig. 4. The morphology of the CDHA powder is needle shaped and mostly agglomerated. The particles are of dimensions: length 16–39 nm and width 7–16 nm. The SAED pattern shows diffused rings, which again confirms nanocrystallinity of CDHA. The inter-planar spacing calculated using the SAED was found to be similar to that of XRD of as synthesized CDHA and HA (JCPDS 9-432) as shown in Table II. This again substantiates the formation of CDHA.

TABLE II The inter-planar spacing of as synthesized CDHA

	Inter-planar spacing (Å)		
	HA	as synthesized CDHA	
Miller indices	JCPDS 9-432	XRD	SAED
(002)	3.44	3.40	3.34
(210)	3.08	3.07	3.02
(211)	2.81	2.81	2.68
(311)	2.15	2.15	2.17
(213)	1.84	1.85	1.88
(410)	1.78	1.77	1.76

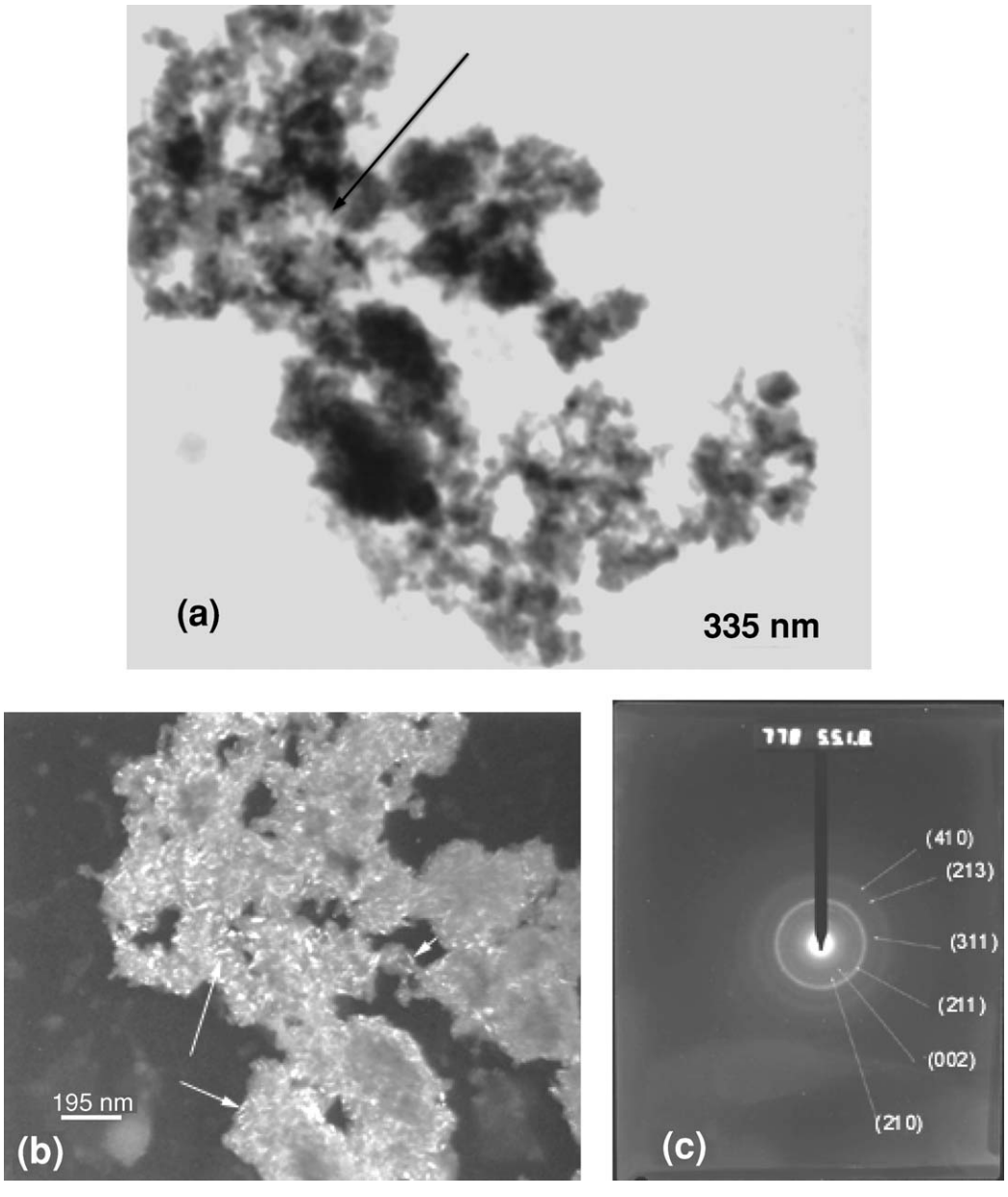

Figure 4 TEM micrograph of as synthesized CDHA: (a) bright field image, (b) dark field image, and (c) SAED pattern.

4. Conclusions

Microwaves were used to accelerate the formation of CDHA with a shorter processing time as compared to other available methods reported. Characterization of CDHA was done by XRD, FT-IR and FT-Raman methods. The TEM study confirms the nanocrystalline nature of synthesized powder having needle-like morphology with length 16–39 nm and width 7–16 nm. The HPO_4^{2-} ions present in CDHA sample converts to $P_2O_7^{4-}$ at temperature around 500°C. The CDHA transforms to β-TCP at around 650°C.

Acknowledgments

The author, A. Siddharthan, thank Mr. Varadachari, Mr. Umapathy, Mrs. Lalitha and Mrs. Kanchanamala for their help in characterization measurements.

References

1. L. L. HENCH, *J. Amer. Ceram. Soc.* **74** (1991) 1487.
2. P. DUCHEYNE, S. RADIN and L. KING, *J. Biomed. Mater. Res.* **27** (1993) 25.
3. C. A. VACANTI and L. J. BONASSAR, *Clin. Orthop.* **367** (1999) S375.
4. SZ-CHIAN LIOU, SAN-YUAN CHEN and DEAN-MO LIU, *Biomaterials* **24** (2003) 3891.
5. L. WINAND, *Ann. Chim. Ser.* **13** (1961) 941.
6. ANNE MORTIER, JACQUES LEMAITRE and PAUL G.ROUXHET, *Thermochimica Acta* **143** (1989) 265.
7. O. R. TRAUTZ, *Ann. New York Acad. Sci.* **60** (1955) 696.
8. M. M. MONTEIRO, N. C. C. ROCHA, A. M. ROSSI and G. A. SOARES, *J. Biomed. Mater. Res.* A **65** (2003) 299.
9. R. Z. LEGEROS, J. P. LEGEROS, G. DACULSI and R. KIJKOWSKA, in "Encyclopedic Handbook of Biomaterials and Bioengineering," edited by Wise DL *et al*. (Markel Dekker, New York, 1995) Vol. 2, p. 1429.
10. P. KASTEN, R. LUGINBUHL, VAN GRIENSVEN, BARKHAUSEN, C. KRETTEK, M. BOHNER and U BOSCH, *Biomaterials* **24** (2003) 2593.
11. M. ANDRES-VERGES, C. FERNANDEZ-GONZALEZ, M. MARTINEZ-GALLEGO, J. D. SOOLIER, CACHADINA and E. MATIJEVIC, *J Mater. Res.* **15** (2000) 2526.
12. YONG HAN, KEWEI XU, GILLAUME MONTAY, TAO FU and JIAN LU, *J. Biomed. Mater. Res.* **60** (2002) 511.

13. ANNE MORTIER, JACQUES LEMAITRE, LUC RODRIQUE and PAUL G ROUXHET, *J. Solid State Chem.* **78** (1989) 215.
14. M. ANDRES-VERGES, C. FERNANDEZ-GONZALEZ and M. MARTINEZ-GALLEGO, *J. Eur. Ceram. Soc.* **18** (1998) 1245.
15. J. RAO, B. VAIDHYANATHAN, M. GANGULI and P. A. RAMAKRISHNAN, *Chem. Mater.* **11** (1999) 882.
16. T. S. SAMPATH KUMAR, I. MANJUBALA and J. GUNASEKARAN, *Biomaterials* **21** (2000) 1623.
17. A. L. MACIPE, J. G. MORALES and R. R. CLEMENTE, *Acta Mater.* **10** (1998) 49.
18. L. B. KONG, J. MA and F. BOEY, *J. Mater. Sci. Mater Med.* **37** (2002) 1131.
19. OHTA, M. YASUDA and H. OKAMURA, *Radiat. Protect. Dosimetry* **94** (2001) 385.
20. A. YOUNG and D. W. HOLCOMB, *Calcif. Tissue Int.* **34** (1982) S17.
21. S. KOUTSOPOULOS, *J. Biomed. Mater. Res.* **62** (2002) 600.
22. R. M. WILSON, J. C. ELLIOT and S. E. P. DOWKER, *J. Solid State Chem.* **174** (2003) 132.
23. R. N. PANDA, M. F. HSIEH, R. J. CHUNG and T. S. CHIN, *J. Phys. Chem. Solids* **64** (2003) 193.
24. A. HADRICH, A. LAUTIE and T. MHIRI, *Spectrochima Acta* **57A** (2001) 1673.

Received 28 January 2004
and accepted 23 June 2004